



Wind Power Ramp Identification based on Continuous Wavelet Transform

Sathish Vijayaraghavalu Haridoss^{1,2,3}, Matthew S. Mason² and Somnath Baidya Roy³

Sathish Vijayaraghavalu
Haridoss

¹University of Queensland –
IIT Delhi Research Academy

s.vijayaraghavaluharidoss@
uqconnect.edu.au

Matthew S. Mason

²School of Civil Engineering,
The University of Queensland

matthew.mason@uq.edu.au

Somnath Baidya Roy

³Centre for Atmospheric
Sciences, Indian Institute of
Technology Delhi

drsbr@cas.iitd.ac.in

ABSTRACT

Wind power generation is greatly affected by the prevailing weather conditions. The intermittent nature of wind energy poses stability challenges in the power grid. A critical aspect of grid stability is the effective management of ramps in wind power. A Wind Power Ramp is a sudden variation in wind power over a short period of time and can be classified as a ramp-up or ramp-down if the power change is positive or negative, respectively. The quantitative definition of a wind power ramp is, however, not universal and several techniques exist for identifying them. Initial studies of wind power ramp detection used binary, threshold-crossing method but were found ineffective when there is significant variability in ramp time scales. To overcome this limitation, the present study explores the use of a Continuous Wavelet Transform (CWT) and random shuffling to identify wind power ramps in 5-minute interval wind power data from the Australian Energy Market Operator. Six wavelets of different vanishing moments are compared for their effectiveness. This comparison reveals that Daubechies-1 and Derivative of Gaussian-1 wavelets exhibit a simple and distinctive pattern in ramp function compared to other wavelets. Daubechies-1 picks ramps of all durations and can identify sub-interval ramps within larger ramps, whereas Derivative of Gaussian-1 is effective only for large duration ramps. Objective evaluation of ramps identified using Daubechies-1 shows that the probability of detection with this technique is 91% for ramp magnitude of at least 30%, and that the ramp duration identified closely matches the actual duration, unlike other wavelets that tend to overestimate this period. Finally, the CWT ramp identification method is applied to a 3-year period of data from the Mt Emerald wind farm to exemplify its use. This shows a seasonally and diurnally varying ramp profile at the site.

INTRODUCTION.

A Wind Power Ramp (WPR) is a sudden variation in wind power over a short period of time. The variation can sometimes last for hours but could be as short as a few minutes. Generally, the ramp is characterized by the magnitude (ΔP), duration (Δt), ramp rate ($\Delta P/\Delta t$) and direction (ramp-up or ramp-down). Both ramp-up and ramp-down ramps destabilise the electrical grid, with the latter being particularly problematic due to the need for reserve power (Zhang et al. 2017). There is no common definition for a ramp because wind farms have varying rated capacity and grid stability is influenced by the region's energy market and pricing. Earlier research on wind power ramp detection employed a binary, threshold-limited approach (DeMarco and Basu 2018). The drawback of this method is that it doesn't cover the diversity in timescale and power change. To overcome this limitation, the Continuous

Wavelet Transform (CWT), a multi-windowed Fourier transform, have been used in many studies as an alternate ramp identification technique (Gallego et al. 2013, Cheneka et al. 2020, Hannesdóttir and Kelly 2019, Pichault et al. 2021). Due to the existence of numerous wavelets, the appropriate choice of wavelet for ramp detection is not immediately clear and the effectiveness of each for detecting wind power ramps has not been systematically investigated. The purpose of this research is to identify the optimal wavelet choice for ramp detection and assess its performance in quantifying ramp parameters, e.g., duration and timing. Once identified, this wavelet will be used to identify and analyse ramps over a 3 year period of 5-minute interval wind power data from the Mt Emerald wind farm in Queensland.

DATA AND METHODOLOGY

Wind Power Data

The Australian Energy Market Operator (AEMO) provides wind power generation data in the form of tables for each wind farm (also other generators) in Australia at 5-minute intervals. The DISPATCH table contains wind power generation data under the column TOTALCLEARED along with the maximum output that a farm can generate under the AVAILABILITY column. The variable TOTALCLEARED is selected to show wind power generation for the current analysis. The data is processed to remove erroneous entries and curtailment periods are excluded for further analysis. Periods of curtailment are identified when (i) there is a semi-dispatch cap and the TOTALCLEARED is less than the AVAILABILITY, or (ii) the Regional Reference Price falls below zero (ARENA 2021). The purpose of this filtering is to exclude wind power ramps that are not related to weather conditions. In this paper, wind power data from the Mt. Emerald wind farm (MEWF) for the period 2019-2021 are used to exemplify the ramp detection method and analysis results.

Ramp Detection Methods

A ramp in a wind power time series is typically identified when there exists a large change in power over a short time period. The adjectives ‘large’ and ‘short’ lack a precise quantitative aspect as it varies depending on the user and the individual application (Ela and Kemper 2009). Given the existence of ramps across various time scales and magnitudes, it is necessary to have a ramp detection approach that can accommodate this variability. In the subsequent section, two techniques of ramp identification are discussed.

Continuous Wavelet Transform and Random Shuffling

Continuous Wavelet Transforms decompose a time series into the time-frequency space and can be used to provide a quantitative measures of ramp characteristics (Gallego et al. 2013). The mathematical expression governing the CWT is,

$$W_p(a, b) = \frac{1}{a} \int_{-\infty}^{+\infty} P(t) \psi\left(\frac{t-b}{a}\right) dt \quad (1)$$

where W_p denotes the wavelet coefficient, a denotes the scales, b denotes the timing, $P(t)$ is the normalised wind power (NWP) time series and ψ denotes the mother wavelet function. Wind power is normalised by dividing the actual power generated by a farm by the total capacity of the wind farm. As scale a relates to the time scale of ramps, a maximum scale of 24 is fixed to analyse ramps with duration up to 3 hours. Previous research has employed either the Daubechies first level (Gallego et al. 2013, Cheneka et al. 2020, Pichault et al. 2021) or the First Derivative of Gaussian (Hannesdóttir and Kelly 2019) wavelet functions. To investigate the effectiveness of these and other distinct wavelets for ramp identification, six wavelet families are investigated here. These include the Daubechies, Symlet, Coiflet, Gaussian, Mexican Hat, and Morlet wavelets. Figure 1 shows an example of the CWT with Daubechies first level wavelet applied to a 24-hour period of normalised wind power data from the MEWF (black solid line). Wavelet coefficients corresponding to wind power ramp periods show higher magnitudes than non-ramp periods and the sign of the wavelet coefficients indicate either ramp up (positive) or ramp down (negative) periods.

While the CWT calculates wavelet coefficient values for all time steps, this doesn't implicitly separate ramp periods from regular periods of power generation. To do this, a process of randomly shuffled surrogates like that used by Cheneka et al. (2020) is applied. In this approach the entire wind power time series is shuffled randomly to make the time series incoherent. The CWT is then applied to obtain surrogate wavelet coefficients $W^*(a,b)$. Cheneka et al. (2020) showed that by using the distribution of $W^*(a,b)$, a wavelet coefficient threshold, $W_T^*(a)$, could be identified to segregate between coherent ramps and random fluctuations in the power signal. To obtain a robust threshold in this process, the random shuffling is performed 100 times and a threshold ($W_T^*(a)$) identified at each scale. A sensitivity study of different threshold discrimination levels (1, 2, 5, 10, 15 and 20 – representing the percentiles at each end of the $W^*(a,b)$ distribution) revealed that the ramp identification and duration most closely matched the manually identified ramps (see next section) when DL was set to 20. This value is thus used here. Therefore, periods where the absolute wavelet coefficient are greater than $W_T^*(a)$ are retained as ramps. In order to determine the ramp duration and timing, a Ramp Function (RF) is defined using Equation 2. This RF, shown as a solid purple line in figure 1, represents the intensity of the ramp event at each time step. Ramp durations are then simply determined by measuring the period of time that has $|RF| > 0$.

$$RF = \frac{1}{a-1} \sum_{a=2}^{a_{max}} W_P(a,b) \quad \text{where } W_P = \begin{cases} W_P(a,b) & \text{if } |W_P(a,b)| \geq W_T^*(a) \\ 0 & \text{elsewhere} \end{cases} \quad (2)$$

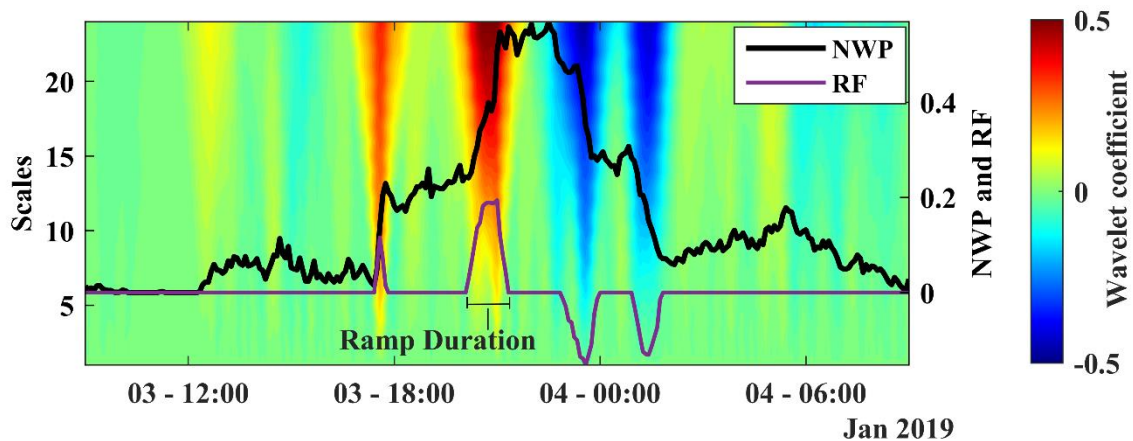


Figure 1. Example of ramps detected by CWT using DB-1 wavelet. Black line represents NWP, purple line is for RF and the colored contour denotes wavelet coefficients. Four ramps are identified between 03 Jan 2019 09:00 and 04 Jan 2019 09:00. All time in AEST.

Manual Ramp Identification

For the purpose of evaluating the efficacy of CWT based ramp detection, ramps are identified manually by visual inspection. A 10 % sample of the MEWF (3-months) wind power time series is chosen for this testing, and a section of the time series is considered part of a ramp if the power change is above 30% and the maximum duration is less than 2 hours (Kiviluoma et al. 2015). Ramps identified manually are considered as a subjective truth, and these ramp events are compared with those from the CWT using a contingency table.

RESULTS AND DISCUSSION

Evaluation of CWT based Ramp Detection

An example of ramps identified in the MEWF time series using the CWT with six different wavelet are compared in Figure 2. Figure 2 shows a 24 hour period of NWP (black solid line) time series and the corresponding RF (coloured lines) of six wavelets along with the time periods of ramps identified

manually (shaded region). The profile of wavelets vary at different levels (i.e., vanishing moments), so only the first level of each wavelet is considered. This decision is based on preliminary analysis, which revealed a complex pattern in RF at levels greater than 1. For the period shown, Daubechies first level (DB-1) and Gaussian first-order derivative (DoG1) wavelets overlap with the region of manually identified ramps, with a positive ramp function for ramp-up and a negative ramp function for ramp-down. The Symlet (SYM) wavelets is inconsistent in its ramp detection even though it overlaps, though not always, with the manual ramp region. Coiflet (COIF) and Morlet (MORL) wavelets on the other hand largely fail to identify ramps over the time series shown. Lastly, the Mexican Hat (MEXH) wavelet, even though it overlaps with manual ramp periods, lacks a distinctive pattern to identify ramps, so was found to be ineffective.

Hannesdóttir and Kelly (2019) used the Gaussian first-order derivative (DoG1) to detect extreme wind speed ramps, but did not explore the effectiveness of this wavelet against DB-1. Here, a comparison between DB-1 and DoG1 ramp durations revealed that DB-1 outperforms DoG1. In many cases, the ramp duration detected by DoG1 overestimates the actual ramp duration, while DB-1 estimates are close to the actual duration. Additionally, DB-1 can detect sub-interval ramps embedded inside a large ramp, which DoG1 fails to identify. The reason that DB-1 performs better than the other wavelets is that it is simply a Harr wavelet having a step function which is what is expected during a ramp.

Using the contingency table, the skill of DB-1 in detecting ramps is assessed. DB-1 successfully identified ramps with a 91% probability of detection (PoD) when the power change exceeded 30%, and the PoD increases with larger power changes. This indicates that CWT with DB-1 is capable of detecting large magnitude ramps. Furthermore, the duration of ramps determined using DB-1 is graphically close to the duration of the ramps in wind power. It can be concluded that DB-1 and DoG1 are appropriate choices for ramp detection. However, DB-1 outperforms DoG1 when assessing their ability to accurately define ramp periods.

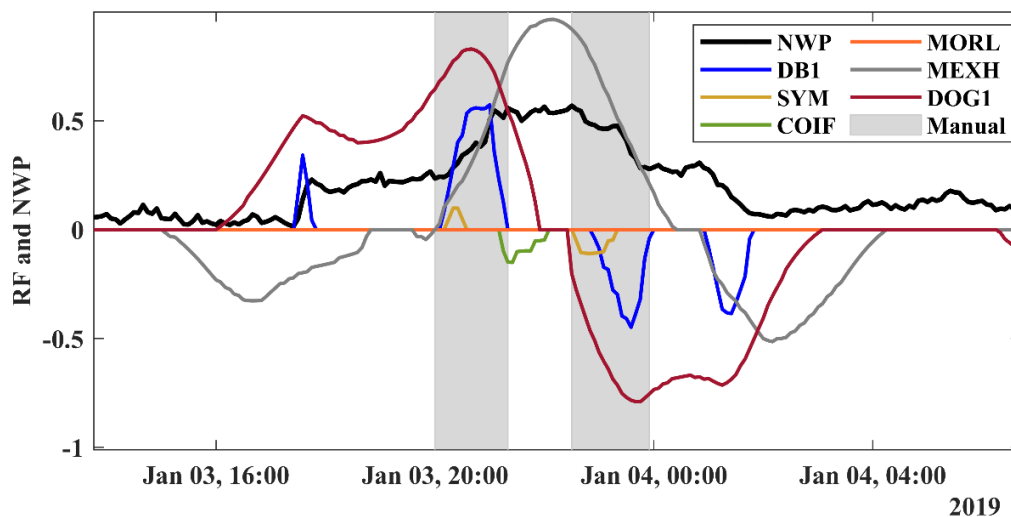


Figure 2. Comparison of CWT based ramp detection with different wavelets.

Characterisation of Ramps

Using the DB-1 wavelet to identify all ramps in the full MEWF time series, the distribution of ramp-rates as a function of ramp duration are shown in figure 3. As can be seen, the sub-hourly ramps are dominant in MEWF. Most frequent ramps occur with ramp-rates (defined as the area under the RF curve for a given ramp divided by its ramp duration) of -0.8 to -1.2 (i.e, ramp-down) and duration of 30-minutes. For ramps lasting up to 1-1.5 hours, there is a linear relationship between ramp-rate and duration. In other words, ramp-rates increases with duration up to 1-1.5 hours and after which it drops down. A similar finding was observed in Cheneka et al. (2020) for Belgian offshore wind farm, but the linear relationship between ramp-rate and duration lasted for up to 12 hours. This difference may be

due to the wind farm capacity, location and the weather system of the region.

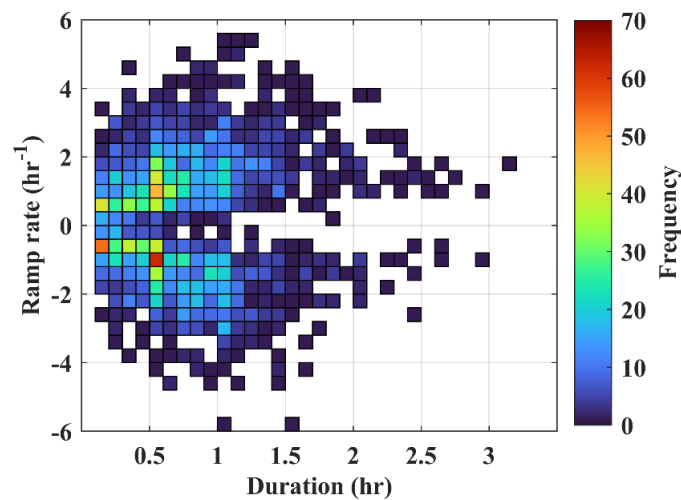


Figure 3. Distribution of ramp-rates and duration with positive (negative) rate for ramp-up (ramp-down)

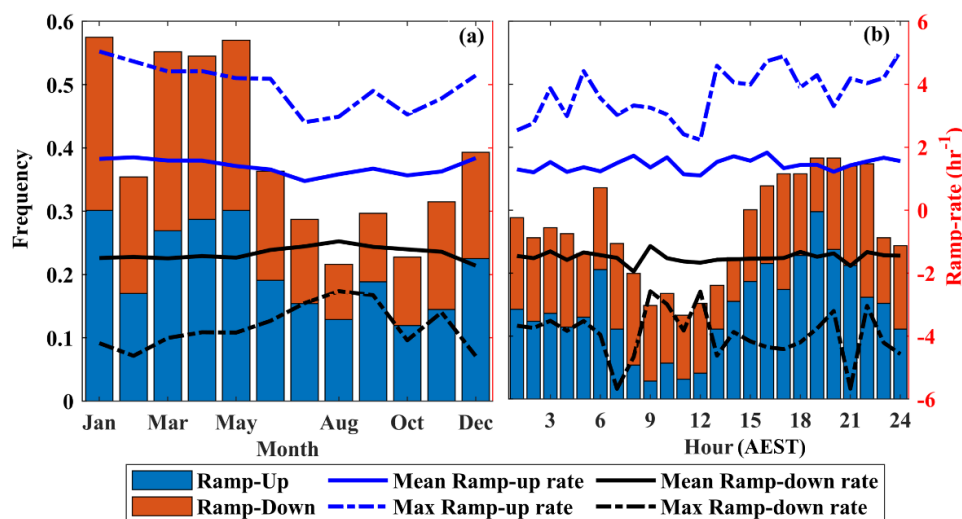


Figure 4. Seasonal (a) and diurnal (b) variation of sub-hourly ramp-ups (blue) and ramp-downs (red) for MEWF. Solid (dashed) line represents mean (maximum) ramp-rates. Blue for ramp-up and black for ramp-down.

As ramps in MEWF occur more frequently in sub-hourly time scale, it is of interest to study the temporal variation of ramps across the day and year. Figure 4a shows the seasonal distribution of sub-hourly ramp-ups and ramp-downs along with the mean and maximum ramp-rate for each month. Both ramp-ups and ramp-downs occur most frequently during Jan-May except for the sharp drop in February. This is believed to be attributed to the Australian monsoon which typically occurs during Oct-April in the region of MEWF. The trend in the mean ramp-rate exhibits a uniform profile throughout the year. However, the ramp-rates are maximum during Dec-May which coincides with the high frequency of ramps during this period. The diurnal distribution of sub-hourly ramp-ups and ramp-downs and the corresponding ramp-rates are shown in figure 4b. A diurnal cycle exists in both ramp-ups and ramp-downs. As the day progress, ramps decrease gradually till noon except for a peak in the early morning, around 06:00. Ramps then starts to rise from noon and reaches its peak during early evening which extends to 22:00. The reason for the peak in the early morning is unknown but the second peak during the evening can be attributed to the turbulent eddies caused by diabatic heating. The mean ramp-rates

are almost uniform throughout the day while maximum ramp-rates occur during the peak ramp occurrence.

CONCLUSIONS

Detection of ramps with a robust method is essential in wind power grid management. The absence of sensitivity tests for ramp detection methods motivates this study and the examination of the effectiveness of a Continuous Wavelet based method with random shuffled surrogates to discriminate ramp events. The use of different wavelets in ramp detection is explored for Mt Emerald Wind Farm and two wavelets are suggested for ramp detection - Daubechies level 1 (DB-1) and First derivative of Gaussian. DB-1 is the recommended choice for ramp detection at fine scales as well as for large scale with 91 % probability of detection and ramp duration close to manual observations. With CWT based ramp detection, distribution of ramp-rates as a function of duration showed the existence of a linear relationship between the ramp-rate and ramp duration for ramps of duration less than 1-1.5 hours. Furthermore, the seasonal variations in ramps revealed the frequent occurrence of ramps during Jan-May. Finally, the existence of a diurnal ramp profile is found with two peaks, one in the early morning and the other during the early evening.

REFERENCES

- AEMO, Nemweb market data, <https://aemo.com.au/en/energy-systems/electricity/national-electricity-market-nem/data-nem/market-data-nemweb>.
- ARENA, The Generator Operations Series: Ramp Rates for Solar and Wind Generators on the NEM, Technical Report, ARENA, August, 2021.
- Bianco, L., Djalalova, I. V., Wilczak, J. M., Cline, J., Calvert, S., Konopleva-Akish, E., Finley, C., and Freedman, J., “A wind energy ramp tool and metric for measuring the skill of numerical weather prediction models”, *Weather and Forecasting*, 31(4), 1137–1156, 2016.
- Cheneka, B. R., Watson, S. J. and Basu, S., “A simple methodology to detect and quantify wind power ramps”, *Wind Energy Science*, 5(4), 1731–1741, 2020.
- Cutler, N., Kay, M., Jacka, K., and Nielsen, T. S., “Detecting, categorizing and forecasting large ramps in wind farm power output using meteorological observations and WPPT”, *Wind Energy*, 10(5), 453–470, 2007.
- DeMarco, A., and Basu, S., “On the tails of the wind ramp distribution”, *Wind Energy*, 21(10), 892–905, 2018.
- Ela, E., and Kemper, J., Wind plant ramping behavior, Technical Report NRE, December, 2009.
- Gallego, C., Costa, A., Cuerva, Á., Landberg, L., Greaves, B., and Collins, J., “A wavelet-based approach for large wind power ramp characterisation”, *Wind Energy*, 16(2), 257–278, 2013.
- Hannesdóttir, Á., and Kelly, M. C., “Detection and characterization of extreme wind speed ramps”, *Wind Energy Science*, 4(3), 385–396, 2019.
- Kiviluoma, J., Holttinen, H., Weir, D., Scharff, R., Söder, L., Menemenlis, N., Cutululis, N. A., Danti Lopez, I., Lannoye, E., Estanqueiro, A., Gomez-Lazaro, E., Zhang, Q., Bai, J., Wan, Y.H., and Milligan, M., “Variability in large-scale wind power generation, *Wind Energy*, 19, 1649–1665, 2015.
- Pichault, M., Vincent, C., Skidmore, G., and Monty, J., “Characterisation of intra-hourly wind power ramps at the wind farm scale and associated processes”, *Wind Energy Science*, 6(1), 131–147, 2021.
- Zhang, J., Cui, M., Hodge, B., Florita, A., and Freedman, J., “Ramp forecasting performance from improved short-term wind power forecasting over multiple spatial and temporal scales”, *Energy*, 122, 528–541, 2017.